

LANGEVIN APPROACH TO UNDERSTAND THE NOISE OF MICROWAVE TRANSISTORS

FABIO PRINCIPATO, BERNARDO SPAGNOLO and GAETANO FERRANTE
*INFM Unità di Palermo and Dipartimento di Fisica e Tecnologie Relative, Università di
 Palermo, Viale delle Scienze, 90128 Palermo, ITALY*

ALINA CADDEMI
*INFM Unità di Messina and Dipartimento di Fisica della Materia e Tecnologie Fisiche
 Avanzate, Università di Messina - Contrada Sperone, 31 - S. Agata, 98166 Messina, ITALY*

Received (July 2003)
 Revised (Oct 2003)
 Accepted (accepted date)

A Langevin approach to understand the noise of microwave devices is presented. The device is represented by its equivalent circuit with the internal noise sources included as stochastic processes. From the circuit network analysis, a stochastic integral equation for the output voltage is derived and from its power spectrum the noise figure as a function of the operating frequency is obtained. The theoretical results have been compared with experimental data obtained by the characterization of an HEMT transistor series (NE20283A, by NEC) from 6 to 18 GHz at a low noise bias point. The reported procedure exhibits good accuracy, within the typical uncertainty range of any experimental determination. The approach allows to extract all the information required for understanding the noise performance of the device without any restriction on the statistics of the noise sources. The results show the relevant noise phenomena from a new angle.

Keywords: Noise modelling, microwave transistor, stochastic integration, HEMT circuit model.

1. Introduction

The noise performance of an active device up to millimeter-wave frequencies plays a basic role in evaluating the suitability of the latter for low-noise applications in advanced telecommunication, nuclear instrumentation and radio astronomy applications. This aspect is gaining increasing importance also due to the implementation of nanometer scale devices where a higher degree of interaction among the intrinsic noise sources is expected to affect the device noise behavior [1]. So far, the noise analysis approaches and the relevant modelling tools employ the representation based on a second order statistics for all the noise sources located inside a transistor [2]. This allows to manage the analytical problems and leads to satisfac-

tory results within the 20 GHz range for device dimensions not aggressively scaled, as for example FET's with gate length not smaller than 0.2 μm .

In this paper we propose a new approach to the problem starting from a general description of all noise sources and solving the stochastic integral equation associated to the equivalent circuit of the microwave device [3]. From the time waveform of the output voltage we obtain the noise figure F as a function of the operating frequency. The noise figure, which is the link between microscopic noise characteristics and macroscopic (i.e. measurable) parameters [4], is calculated by the ratio of the spectral noise power density produced at the output of the noisy device to the spectral noise power density produced at the output of the ideal noiseless device. More specifically, our calculation were performed for a noise source impedance of 50 Ω , but the procedure can be applied for arbitrary impedance value. We determine the device noise figure F_{50} at different discrete frequencies over a given operating range. Then, we compare the values of F_{50} calculated by means the proposed method with data referring to characterization of an HEMT transistor series (NE20283A, by NEC) from 6 to 18 GHz at a low noise bias point [5]. The proposed procedure exhibits fairly good accuracy, within the typical uncertainty range of any experimental determination. It is worthwhile to note that for Gaussian statistics the conventional CAD tools and our approach coincide. However for non-Gaussian noise sources, i.e. when it is important to know higher order statistics, our noise modelling is appropriate. In fact with our approach we can use different statistics of the noise sources and therefore obtain all the moments of the output voltage as a function of the cross-correlation functions of the noise sources. This technique can thus be applied to extract all the information required for a complete knowledge of the noise performance of the device without any restriction on the statistics of the noise sources, including also cross-correlated noise sources.

2. HEMT Circuit Model

High electron mobility transistors (HEMT) are GaAs or In-based field-effect transistors for application at microwave and millimeter wave frequencies. These devices began to set records for noise performance since their introduction in the early '90s and therefore represent key elements in all low-noise circuits. The linear equivalent circuit which typically models the small-signal performance of HEMT's at microwave frequencies is shown in Fig. 1. This circuit represents the chip device because access inductances and parasitic interelectrode capacitances are not included. The values of the circuit elements are usually determined by computer-aided modelling procedures which may follow either optimization-based or direct extraction criteria [6, 7, 5]. More recently, approaches based on artificial neural networks have been successfully employed [8]. We had previously characterized an HEMT transistor series (NE20283A, by NEC) over the 6 – 18 GHz frequency range at the low noise bias conditions suggested by the manufacturer ($V_{DS} = 2.0\text{ V}$, $I_{DS} = 10\text{ mA}$). By microwave measurements, we determined both the scattering and the noise parameters of the packaged device, i.e. the device sealed within a ceramic enclosure equipped with metallic leads. From the experimental data, we extracted a linear noisy model for the whole structure by a variable decomposition approach with a separate tuning for the channel noise source value modelled by

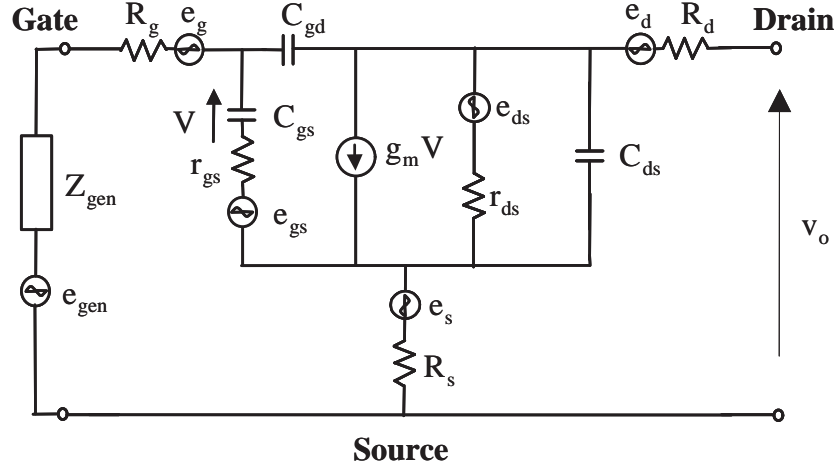


Fig 1. Small-signal circuit model of a chip HEMT with noise sources.

an equivalent noise temperature assigned to the r_{ds} resistor [9]. The values of the circuit elements and the noise temperature T_d so obtained are listed in Tab. 1.

r_{gs} [Ω]	r_{ds} [Ω]	R_g [Ω]	R_d [Ω]	R_s [Ω]	C_{gs} [fF]	C_{gd} [fF]	C_{ds} [fF]	τ [ps]	g_{m0} [mS]	T_d [K]
1.2	274	2.0	0.67	0.55	261	20.0	34.6	0.68	46.2	2250

 Table 1. Values of circuit elements of the chip HEMT model at $V_{DS} = 2.0 V$ and $I_{DS} = 10 mA$.

All the other resistors in the model contribute with thermal noise typical of equilibrium conditions with device environment (i.e. $300K$). The comparison between the noise parameters measured and modelled for the packaged device data was presented in [5]. We here report for the reader's convenience the plot of the noise figure in input matched condition in Fig. 2. To carry out our analysis we employ the model structure representing the chip device so eliminating the effect of the package found to be lossless (i.e. not containing noise sources). Among all noise parameters we use the F_{50} noise figure as information test to check the effectiveness of the procedure here presented. Therefore, the new results are compared with F_{50} data referring to the chip as simulated via CAD by use of the above circuit model.

3. General Noise Analysis by Langevin Approach

For the sake of simplicity and to validate our theoretical approach we suppose that all noise sources in the HEMT model are Gaussian white noise of thermal origin with zero mean, δ -correlated and variance per unit of frequency bandwidth equal to $\sigma^2 = 4kT_xR_x$, where k is the Boltzmann constant, R_x the resistance and T_x the equivalent temperature of the resistor. No correlation is assumed among the noise sources. The noise voltage generator e_{gen} is the thermal noise associated with the real part of

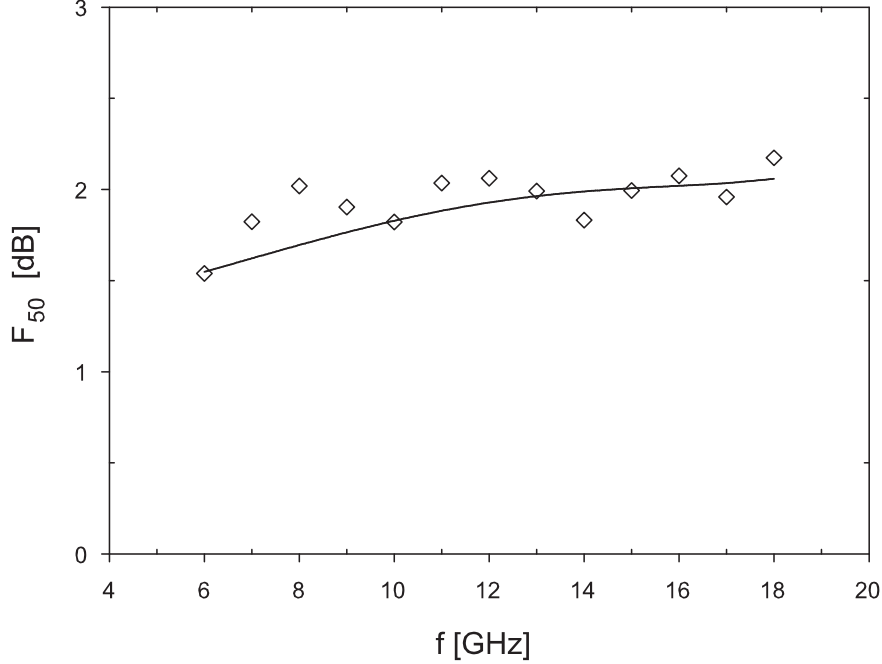


Fig 2. Comparison between the measured noise figure F_{50} of the packaged HEMT transistor series NE20283A by NEC (\diamond) and the F_{50} simulated with CAD ($-$).

the impedance $Z_{gen} = R_{gen} + j\omega X_{gen}$ of the input termination at the reference temperature $T_0 = 290K$, which is the standard temperature to determine the noise figure. The resistances r_{gs} and r_{ds} contribute to noise by assigning equivalent temperature T_g and T_d , respectively. The temperature of the intrinsic gate-source resistance r_{gs} is assumed to be equal to the environment temperature ($T_g = T_0$) [9]. In order to determine the expression of the output noise voltage v_o as a function of the noise sources, the circuit network is analyzed in the Laplace domain. So that we have the Laplace transform of the zero-state (at $t = 0$) response of the output voltage

$$V_o(s) = \sum_{i=1}^6 H_i(s)E_i(s), \quad (1)$$

where s is a complex variable, $H_i(s)$ are the transfer functions from the i -th noise generator to the output, and $E_i(s)$ are the Laplace transforms of the voltage generators with the following notation: $1 \rightarrow e_{gen}$, $2 \rightarrow e_s$, $3 \rightarrow e_d$, $4 \rightarrow e_g$, $5 \rightarrow e_{gs}$ and $6 \rightarrow e_{ds}$. In the equivalent circuit of the HEMT, the small-signal g_m transconductance depends on the variable s as $g_m = g_{m0}e^{-s\tau}$, where g_{m0} is the dc value of the transconductance and τ is the transit time of the carriers to diffuse from source to drain. Since the value of τ is a fraction of picosecond, and we are inter-

ested in investigating the frequency range below 20 GHz, where $|s = i\omega| \ll \frac{1}{\tau}$, we approximate the exponential function as $e^{-s\tau} \simeq 1 - s\tau + \frac{1}{2}(s\tau)^2$. Consequently the $H_i(s)$ are rational functions of the complex variable s . By anti-transforming (1), we obtain the zero-state response of the output voltage in the time domain which assume the expression valid for $t > 0$

$$v_o(t) = \sum_{i=1}^6 \int_0^t h_i(t-t') e_i(t') dt', \quad (2)$$

where the function $h_i(t)$ are the impulse responses corresponding to the $H_i(s)$, which assume the expression

$$h_i(t) = h_{i0}\delta(t) + h_{i1}e^{-\frac{t}{\tau_1}} + h_{i2}e^{-\frac{t}{\tau_2}} + h_{i3}e^{-\frac{t}{\tau_3}}, \quad t > 0. \quad (3)$$

Here $\delta(t)$ is the Dirac δ -function. The time constants τ_i of the impulse response and the coefficients h_{ij} depend on the circuit parameters and are obtained from the poles of the network functions $H_i(s)$ (see Appendix A). For the investigated model the following inequalities are satisfied

$$\tau_3 \ll \tau_1\tau_2 \quad \text{and} \quad \omega \ll \frac{1}{\tau_3}, \quad (4)$$

thus the relation (3) can be approximated as:

$$h_i(t) \approx h_{i0}\delta(t) + h_{i1}e^{-\frac{t}{\tau_1}} + h_{i2}e^{-\frac{t}{\tau_2}}. \quad (5)$$

By using Eqs. (2) and (5) the output voltage of the HEMT model in the time domain can be expressed as the following stochastic integral equation in the Ito sense

$$v_o(t) = \sum_{i=1}^6 [h_{i0} e_i(t) + \int_0^t h'_i(t-t') e_i(t') dt'], \quad (6)$$

where the function h'_i contains only the last two terms of the expression (5). The Eq.(6) is the main result of our paper. It gives the stochastic output voltage of the HEMT device as a function of the different stochastic processes which represent the noise sources. By inserting the different statistics of the noise sources in Eq.(6) we can extract all the moments of the output voltage $v_o(t)$ required for a complete knowledge of the noise performance when higher order statistics occurs in the output signal of the devices. As an example we report in Appendix B the expression of the second moment and the general expression of the n th moment of the output voltage as a function of the cross-correlation functions of the noise sources. As a first step of investigations and to validate our stochastic approach we consider all noise generators $e_i(t)$ present in the model as uncorrelated Gaussian white noises, with the usual statistical properties: $\langle e_i(t) \rangle = 0$ and $\langle e_i(t) e_i(t') \rangle = \sigma_i^2 \delta(t-t')$. Here σ_i^2 is the variance per unit of frequency bandwidth of the i -th generator. Therefore the time waveform of the output voltage can be obtained by numerical integration of Eq. (6). In Eq. (6) the terms $e_i(t) dt = dW_i(t)$ are Wiener processes associated with the device noise sources [10]. The numerical simulation of Eq.(6) is performed

by choosing the time step $\Delta t = \min\{\tau_1, \tau_2\}/10$, in order to prevent aliasing. At each temporal step $t_n = n \Delta t$, by using the algorithm for Gaussian random variables [11], the Wiener increments are calculated as $\Delta W_i(t_n) = \sigma_i \xi(t_n) \sqrt{\Delta t}$. The digital implementation of the impulse response (5) allows to calculate the output voltage by the discrete-time convolution between the sequences $h'_i(t_n)$ and the noise sources $e_i(t_n)$

$$\sum_{i=1}^6 \sum_{k=0}^n h'_i(t_{n-k}) \Delta W_i(t_k). \quad (7)$$

The duration of the sequence $h'_i(t_n)$ increases with n , therefore we consider only the first n_{max} terms of the sequence $h'_i(t_n)$ to save computation time. That is

$$v_o(t_n) = \sum_{i=1}^6 \sum_{k=n-n_{max}}^n [h_{i0} e_i(t_n) + h'_i(t_{n-k}) \Delta W_i(t_k)]. \quad (8)$$

The time discretization and the finite duration of the impulse response (FIR) introduce an error. In order to evaluate this error the z-transform of the sequence $h_i(t_0), h_i(t_1), h_i(t_2), \dots, h_i(t_{n_{max}})$ is considered

$$H_{di}(z) = \sum_{n=0}^{n_{max}} h_i(t_n) z^{-n}. \quad (9)$$

The error is evaluated by comparing the module of the Fourier transform of the continuous transfer function, i.e.

$$H_i(i\omega) = h_{i0} + \frac{h_{i1}}{1/\tau_1 + i\omega} + \frac{h_{i2}}{1/\tau_2 + i\omega}, \quad (10)$$

with the Fourier transform of the sequence $h_i(t_n)$, i.e. $H_{di}(z = e^{i\omega\Delta t})$, at different values of n_{max} and for each generator e_i . The comparison between the continuous and the discrete transfer function is shown in Fig. 3, where we report the normalized Fourier transform of the transfer function versus the normalized frequency. In this figure we use $n_{max} = m \times \max\{\tau_1, \tau_2\}$, with m integer, and $f_s = 1/(2\Delta t)$ is the Nyquist frequency. As m increases, the difference between continuous and the approximate impulse response becomes negligible. At $m = 6$ the error introduced by the FIR impulse response are less than 1%. We use this value of m in our simulations.

4. Results

The samples of the output noise voltage waveforms were calculated for an input termination 50Ω from Eq. (8) by using C-language routines. To validate the approach proposed in this paper we compare the theoretical results of the noise figure F_{50} with that obtained by CAD analysis in the 6-18 GHz frequency range. The temporal noise sequence was generated by using a time step Δt of 5.57×10^{-13} sec and Gaussian random number generator. The Nyquist frequency is 0.898 THz,

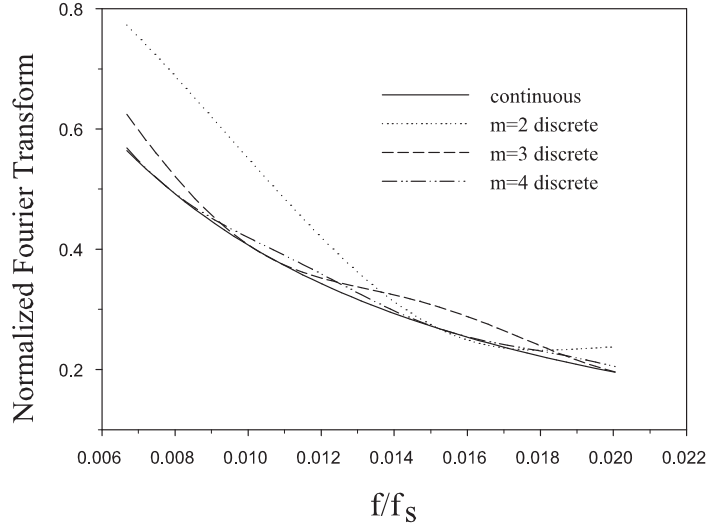


Fig 3. Normalized module of the Fourier transform of the transfer function from the input generator to voltage output for the continuous and discrete impulse response and for different values of the integer m . In the x-axis the frequency is normalized with respect to the Nyquist frequency and the values are restricted to the 6 – 18 GHz frequency band.

thus $N = 10^5$ points are needed at least to investigate the microwave frequency range. The noise figure is calculated by using the following relation [12]:

$$F_{50} = \frac{p_{on}(f)}{p_{off}(f)} \quad (11)$$

where $p_{on}(f)$ is the power spectral density of the output voltage at the frequency f when all the noise sources are activated and $p_{off}(f)$ is the power spectral density obtained from the noise source of the input termination only, both in V^2/Hz units. In order to improve the estimation of the spectral power density given by (11) at a given value of frequency \bar{f} , we use the mean value of the noise power evaluated within the frequency bandwidth BW around \bar{f}

$$\langle p_x(\bar{f}) \rangle = \frac{1}{BW} \int_{\bar{f}-BW/2}^{\bar{f}+BW/2} p_x(f) df. \quad (12)$$

The output noise waveforms of the HEMT model, with (v_{on}) and without (v_{off}) the internal noise sources, over a sample time interval of 20 ns are reported in Fig. 4. The total time period used for calculation is $N \Delta t$, where N is usually chosen to be 1×10^5 .

By using $BW = 90$ MHz for noise power estimation, we calculate the F_{50} as a function of the operating frequency in the 6-18 GHz range. In Fig. 5 we compare the noise figure behavior obtained with our approach with that obtained by computer-aided analysis of the model.

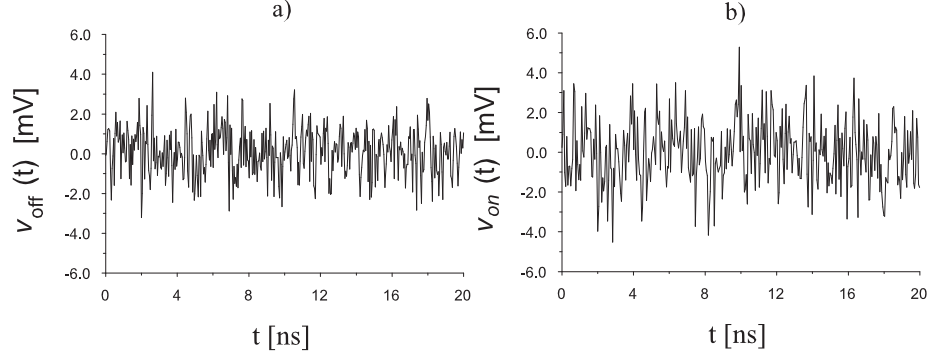


Fig 4. Output noise waveforms of the HEMT model without v_{off} (a) and with v_{on} (b) internal noise sources.

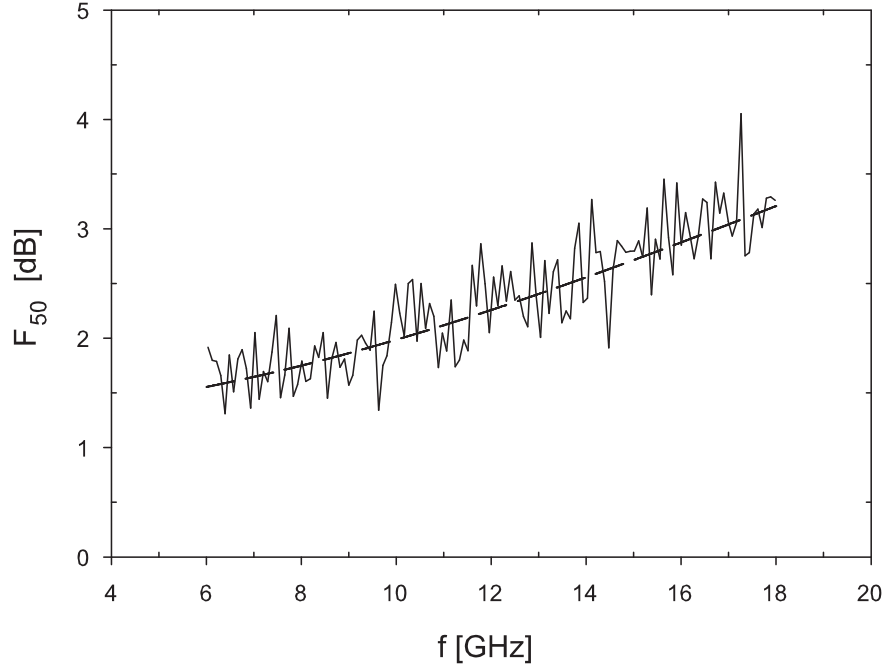


Fig 5. Noise figure F_{50} calculated with Langevin approach and by using $BW = 90$ MHz for noise power estimation (—) compared with F_{50} obtained by computer-aided analysis of the model (--).

Good agreement is exhibited by the two noise figure curves. We use 100 realizations of time waveforms to determine each noise figure behavior over the given frequency range. The results obtained with the stochastic approach may be improved by averaging over a greater number of realizations but with more computer time consuming. We note that the noise figure behavior obtained with the stochastic approach could be thought as the output of a noise figure measuring instrument where averaging and smoothing options are available to minimize display jitter. The procedure here described can be used with any input termination value to obtain more than one noise figure value. By choosing four different termination values, the extraction of all the standard noise parameters can be performed by using the equation

$$F(\Gamma_{gen}) = F_0 + 4r_n \frac{|\Gamma_{gen} - \Gamma_o|^2}{|1 + \Gamma_o|^2(1 - |\Gamma_{gen}|^2)} \quad (13)$$

where Γ_{gen} is the generic termination value expressed in a reflection coefficient form and F_0 , Γ_o (magnitude and angle) and r_n are the four noise parameters usually determined by complex experimental procedures [13].

By calculating the noise parameters vs. frequency, a complete knowledge of the noise behavior of any two-port is obtained from a circuit point of view. The noise parameters can be employed either for extraction of device intrinsic noise sources or for CAD of low-noise circuits.

5. Conclusions

We have presented a noise analysis procedure for microwave transistors. This procedure is based on Langevin approach and takes the general statistical properties of the internal noise sources into account. The device is represented by its equivalent circuit with noise generators to a chip level. The noise figure at a given input termination is determined by first integrating the noise voltage equations in the time domain and by transforming them into spectral power densities over the frequency range of interest. The results are compared with the simulated data, obtained with a commercial CAD, of the chip model of an HEMT device series (NE20283A, by NEC) from 6 to 18 GHz at a low noise bias point. The proposed procedure exhibits good accuracy within the typical uncertainty range of any experimental determination. Our Langevin approach gives the same results of noise analysis approaches based on second order statistics. But when higher order statistics becomes relevant to the noise analysis our approach is suitable. Moreover the cross-correlation functions between the noise sources of the device are explicitly included in our theoretical approach (see Appendix B), while in conventional CAD methods they are inserted in a heuristic way. Such a general approach can be extended to analyze noise in other devices without restrictions as to the frequency range, by specifying the device equivalent circuit and the statistical properties of the internal noise sources.

Acknowledgements

The authors are grateful to Dr. D. Valenti for helpful discussions concerning simulation. This work was supported by the National Institute for the Physics of

Matter (I.N.F.M.), by INTAS Grant 01-450 and by Italian Ministry of University and Research (MIUR).

References

- [1] *Noise and Fluctuations Control in Electronic Devices*, ed. A. A. Balandin, Am. Sc. Pub. (2002), Los Angeles, California, USA.
- [2] W. Marshall Leach Jr., *Fundamentals of Low-Noise Analog Circuit Design, Proceedings of the IEEE*, **82** (1994), 400–433.
- [3] A preliminary account has been presented at *16th International Conference on Noise in Physical Systems and 1/f Fluctuations, Gainesville, Florida, USA, October 22-25, Proc. World Sc., ed. Bosman, pp. 221-224, 2001.*
- [4] H.T. Friis, *Noise Figure of Radio Receivers, Proceedings of the IRE*, **32** (1944), 419–422.
- [5] A. Caddemi, A. Di Paola, M. Sannino, *Full Characterization of Microwave Low-Noise HEMT's: Measurement vs. Modeling, IEEE Trans. on Instrumentation and Measurement*, **46** (1997), 1–5.
- [6] C. Van Niekerk, P. Meyer, *Performance and Limitations of Decomposition-Based Parameter Extraction Procedures for FET Small-Signal Models, IEEE Trans. Microwave Theory Tech.*, **46** (1998), 1620–1627.
- [7] A. Caddemi, N. Donato, *On the Noise Resistance of Field-Effect Transistors at Microwave Frequencies, Fluctuations and Noise Letters*, **1**, (2001), 151–161.
- [8] V.K. Devabhaktuni, M. Yagoub, Q.J. Zhang, *A Robust Algorithm for Automatic Development of Neural-Network Models for Microwave Applications, IEEE Trans. Microwave Theory Tech.*, **49** (2001), 2282–2290.
- [9] M. Pospieszalski, *Modeling of Noise Parameters of MESFETs and MODFETs and their Frequency and Temperature Dependence, IEEE Trans. Microwave Theory Tech.*, **37** (1989), 1340–1350.
- [10] C.W. Gardiner, *Handbook of Stochastic Methods*, cap. 4, Springer-Verlag, Berlin, (1985).
- [11] W. H. Press et al., *Numerical Recipes in C: The Art of Scientific Computing*, cap. 7, Second Edition, Cambridge, University Press, (1992).
- [12] F. Principato, G. Ferrante and R. N. Mantegna, *A Method for the Analytical Calculation of Noise Parameters of Linear Two-Ports with Crosscorrelated Noise Sources, IEEE Trans. on Circuits and Systems-I*, **46**, (1999), 1019–1022.
- [13] G. Martines, M. Sannino, *The Determination of the Noise, Gain and Scattering Parameters of Microwave Transistors using only an Automatic Noise Figure Test Set, IEEE Trans. Microwave Theory Tech.*, **42** (1994), 1105–1113.

Appendix A.

Because of the topological complexity of the HEMT model network it is not possible to obtain the expression of the time constants τ_i in a closed form. Indeed the τ_i are obtained from the poles of the transfer function $H_i(s)$, which are the roots of the third-order algebraic equation

$$2(1 + (C_{gs}r_{gs} + C_{gd}r_{ds} + C_{ds}r_{ds} + C_{gs}R_g + C_{gd}R_g + R_{gen}C_{gd} + R_{gen}C_{gs} + g_{m0}r_{ds}C_{gd}R_g + R_sC_{gs} + g_{m0}R_sr_{ds}C_{gd} + R_sC_{gd} + g_{m0}r_{ds}C_{gd}R_{gen})s$$

$$\begin{aligned}
 & + (C_{ds}r_{ds}C_{gs}r_{gs} + C_{ds}r_{ds}C_{gd}R_g + C_{gd}r_{ds}C_{gs}R_g + C_{ds}r_{ds}C_{gs}R_g + C_{gs}r_{gs}C_{gd}R_g \\
 & - g_{m0}r_{ds}\tau C_{gd}R_g + r_{ds}C_{gs}r_{gs}C_{gd} + R_sC_{ds}r_{ds}C_{gd} + R_sr_{ds}C_{gs}C_{gd} + R_sC_{ds}r_{ds}C_{gs} \\
 & + r_{gs}R_sC_{gs}C_{gd} - g_{m0}R_sr_{ds}\tau C_{gd} + C_{gd}r_{ds}R_{gen}C_{gs} + C_{ds}r_{ds}R_{gen}C_{gs} \\
 & + C_{ds}r_{ds}R_{gen}C_{gd} + C_{gs}r_{gs}C_{gd}R_{gen} - g_{m0}r_{ds}\tau C_{gd}R_{gen}) s^2) \\
 & + (C_{gd}r_{ds} (g_{m0}\tau^2 + 2r_{gs}C_{gs}C_{ds}) (R_g + R_s + R_{gen})) s^3 = 0.
 \end{aligned} \tag{A.1}$$

Appendix B.

In the HEMT model the only plausible cross-correlated noise sources are the gate-source e_{gs} and the drain-source e_{ds} [9]. Do to this hypothesis we obtain from Eq. (6) the general expression for the second moment of the output voltage $v_0(t)$ as a function of the cross-correlation function between the e_{gs} and the e_{ds} noise sources

$$\begin{aligned}
 \langle v_0^2(t) \rangle &= \sum_{k=0}^6 h_{i0}^2 \sigma_i + 2 h_{50} h_{60} \langle e_5(t) e_6(t') \rangle + \sum_{k=0}^6 \int_0^t h_i'^2(t-t') \sigma_i dt' \\
 &+ 2 \int_0^t \int_0^t h_5'(t-t') h_6'(t-t'') \langle e_5(t') e_6(t'') \rangle dt' dt'' + \sum_{k=0}^6 h_{i0} h_i'(0) \sigma_i \\
 &+ h_{50} \int_0^t h_5'(t-t') \langle e_5(t) e_6(t') \rangle dt' + h_{60} \int_0^t h_6'(t-t') \langle e_6(t) e_5(t') \rangle dt,
 \end{aligned} \tag{B.2}$$

where we use the property of the Dirac δ -function. The general expression of the moments of $v_0(t)$ with the same above-mentioned hypothesis is

$$\begin{aligned}
 \langle v_0^n(t) \rangle &= \sum_{k=0}^n \sum_{g=0}^{(n-k)} \sum_{j=0}^{(n-k-g)} \sum_{l=0}^{(n-k-g-j)} \sum_{p=0}^{(n-k-g-j-l)} \binom{n}{k} \binom{n-k}{g} \binom{n-k-g}{j} \\
 &\binom{n-k-g-j}{l} \binom{n-k-g-j-l}{p} \langle \sum_{m=0}^k \binom{k}{m} \left[\int_0^t h_6'(t-t') e_6(t') dt' \right]^m \\
 &\cdot (h_{60} e_6(t))^{k-m} \sum_{q=0}^g \binom{g}{q} \left[\int_0^t h_5'(t-t') e_5(t') dt' \right]^q (h_{50} e_5(t))^{g-q} \rangle \\
 &\cdot \sum_{r=0}^j \binom{j}{r} \langle \left[\int_0^t h_4'(t-t') e_4(t') dt' \right]^r (h_{40} e_4(t))^{j-r} \rangle \\
 &\cdot \sum_{s=0}^l \binom{l}{s} \langle \left[\int_0^t h_3'(t-t') e_3(t') dt' \right]^s (h_{30} e_3(t))^{l-s} \rangle \\
 &\cdot \sum_{u=0}^p \binom{p}{u} \langle \left[\int_0^t h_2'(t-t') e_2(t') dt' \right]^u (h_{20} e_2(t))^{p-u} \rangle
 \end{aligned}$$

$$\begin{aligned}
 & \cdot \sum_{z=0}^{(n-k-g-j-l-p)} \binom{n-k-g-j-l-p}{z} \\
 & \cdot \left\langle \left[\int_0^t h_1'(t-t') e_1(t') dt' \right]^z (h_{10} e_1(t))^{(n-k-g-j-l-p)-z} \right\rangle
 \end{aligned}
 \tag{B.3}$$